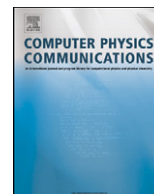




Contents lists available at ScienceDirect

Computer Physics Communications

www.elsevier.com/locate/cpc

A metaheuristic approach to the optimal definition of molecule-fixed axes in rovibrational Hamiltonians

M.E. Castro, A. Niño, C. Muñoz-Caro*

Grupo de Química Computacional y Computación de Alto Rendimiento, Escuela Superior de Informática, Universidad de Castilla-La Mancha, Paseo de la Universidad 4, 13071 Ciudad Real, Spain

ARTICLE INFO

Article history:

Received 25 August 2009

Received in revised form 2 December 2009

Accepted 25 January 2010

Available online xxxx

Keywords:

Rovibrational Hamiltonian

Rotation-vibration coupling

G matrix

Simulated annealing

ABSTRACT

We develop an algorithmic, metaheuristic approach to the definition of molecule-fixed axes orientation in molecules of arbitrary size. The goal is to simplify the treatment of overall rotation and rotation-vibration interaction in rovibrational Hamiltonians. Considering the kinetic elements of the rovibrational Hamiltonian, given by the \mathbf{G} matrix, we select the optimal orientation of molecule-fixed axes minimizing specific \mathbf{G} matrix elements. To such an end, we develop a global minimization method based in a hybrid Simulated Annealing + Powell's local minimization. The parameters of the method are calibrated using a set of non-rigid molecules: Acetaldehyde, glycolaldehyde, methyl formate and ethyl methyl ether. The results show that the principal axes of inertia do not give the simplest form to the pure rotational contribution. However, minimization of the \mathbf{G} matrix rotational element does. Finally, we observe that in the cases considered it is not possible to nullify all the rotation-vibration coupling elements, since the torsional motions are coupled with the overall rotation. However, the treatment yields the optimal solution. The methodology proposed allows also to simplify simultaneously the pure rotational + rotation-vibration coupling elements in rovibrational Hamiltonians.

© 2010 Published by Elsevier B.V.

1. Introduction

Rotation-vibration, rovibrational, data provide invaluable information about molecular structure, potential energy surfaces, reactivity and internal dynamics of molecules. The experimental information, usually in the form of spectra, needs interpretation by enough accurate theoretical models properly describing molecular rotation and vibration. Models able to describe the observed data can be used to generate new information not yet experimentally available. Therefore, the building of molecular rovibrational Hamiltonians is a topic of interest since the first times of quantum mechanics.

When building a molecular rovibrational Hamiltonian, a series of steps should be followed [1-4]. First, we define the positions of the nuclei of the molecule using a laboratory-fixed Cartesian axes system. To separate the effect of translation, a new set of space-fixed axes, parallel to the laboratory system, is placed at the center of mass of the molecule. In addition, to introduce rotational coordinates, a new molecule-fixed axes system, also centered at the center of mass but rotating with the molecule, is defined. Finally, the Euler angles [5] are used as rotation coordinates specifying the orientation of the molecule-fixed axes respect to the space-fixed axes. The last step is to define a set of vibrational coordinates for the nuclei in the molecule. These coordinates must be invariant under translation and rotation. In this form, the potential function only depends on these coordinates. This simplifies the resolution of the rovibrational Hamiltonian. The result is that the rovibrational coupling appears only in the kinetic operator of the Hamiltonian. In turn, the kinetic operator can be defined in terms of the rovibrational \mathbf{G} matrix, or tensor [6-8]. The \mathbf{G} matrix collects the overall rotation and the pure vibrational contributions, as well as the rotation-vibration interaction (Coriolis term). Since the rovibrational coupling mixes rotation and vibration coordinates, its removal, or at least minimization, is of great interest when defining methods to solve the rovibrational Hamiltonian. To such an end, the most appropriate orientation of the molecule-fixed axes respect to the space-fixed system must be used.

Two classical cases exemplify the use of well selected molecule-fixed axes. In the simplest case, we use an orientation that diagonalizes the inertial tensor, \mathbf{I} . Thus, the non-diagonal elements of \mathbf{I} are zeroed or, in other words, they are minimized. The corresponding axes are the principal axes of inertia, and the diagonal elements of the inertial tensor are the principal moments of inertia [5]. The solution is the simplest respect to pure rotation, but the rovibrational coupling is not taken into account. On the other hand, it is possible to consider

* Corresponding author. Tel.: +34 926295362; fax: +34 926295354.
E-mail address: camelia.munoz@uclm.es (C. Muñoz-Caro).

specifically the rovibrational coupling. Thus, assuming the nuclei to perform very small amplitude vibrations around the equilibrium position, the molecule-fixed axes orientation can be determined by imposing the Eckart conditions [9,10]. These conditions represent the cancellation of the angular momentum at the equilibrium. Therefore, the rovibrational coupling at that point is zero, and small around it. For very small amplitude motions this is a good approximation. In fact, the **well-known** rectilinear normal coordinates are defined for a quadratic potential using this approach [1]. A more realistic approach is to allow displacements beyond the quadratic zone of the potential energy. Thus, the standard treatment of semi-rigid molecules, as worked out by Wilson and Howard [11], and Darling and Dennison [12] and simplified by Watson [13,14], uses normal modes to express the rovibrational Hamiltonian. This Hamiltonian, known as the Watsonian, applies the Eckart conditions to define the molecule-fixed coordinates system. The relationship between Eckart axes and the minimization of the root-mean-square deviation with respect to the molecule-fixed axes has been considered recently [15].

From a different standpoint, a series of works, proposing symplectic integration methods for molecular dynamics, have been reported [16–20]. In these works, normal modes are used to solve the classical Hamilton equations of motion. In addition, all types of motions are described in terms of normal coordinates, with translation and rotation treated as zero frequency vibrations. Eckart axes are used as molecule-fixed axes. Using this approach, IR spectra can be computed by a Fourier transform of the dipole moment autocorrelation function [19].

Whereas discussion of suitable sets of internal, vibrational coordinates has been an active topic, see for instance Ref. [21], additional efforts to define new molecule-fixed axes orientations are scarce in the literature. Thus, in the **well-known** work by Hougen, Bunker and Johns [22] on triatomic molecules, the Eckart conditions are used to simplify the Coriolis coupling for the rectilinear coordinates and a single large amplitude motion. On the other hand, the work by Sutcliffe and Tennyson [23] on triatomic molecules represents an interesting contribution. Here, the Euler angles are chosen in terms of three rotationally invariant internal coordinates. In addition, Wei and Carrington [24,25] tried to combine in triatomic molecules the virtues of the Eckart conditions with that of internal orthogonal coordinates. Also, it is worth to mention the work of Makarewicz and Bauder [26]. These authors proposed a numerical method to minimize, in non-rigid molecules, the Coriolis coupling for selected small amplitude vibrations.

Therefore, the definition of a molecule-fixed system in molecules of arbitrary size, which minimizes rovibrational coupling (or more generally, specific elements of the kinetic operator) is a topic not yet fully resolved. At this point, it is important to realize that selection of the most appropriate orientation of the molecule-fixed axes for vibrational studies can be related to the minimization of specific elements of the rovibrational, kinetic, \mathbf{G} matrix. Therefore, metaheuristic, global optimization strategies can be useful in this context. A metaheuristic is a high level general strategy, which guides others (heuristics) to search for feasible solutions in complex domains. Examples of metaheuristics are simulated annealing, genetic algorithms and Tabu Search [27]. In particular, simulated annealing (SA) [27, 28] is simple to implement and, if appropriately calibrated, more efficient (fewer number of evaluations of the target or cost function) than a brute-force exploration of the problem definition space. The name of this metaheuristic comes by analogy with the annealing process in metallurgy. This process consists in heating a metal at a very high temperature so that its atoms are placed above any local internal energy minimum. Then, the temperature is slowly lowered, allowing the atoms to locate and finally remain in the global internal energy minimum. They were **Kirkpatrick** et al. [29] who proposed SA as an approach for the computation of the global minimum in arbitrary functions. SA uses the Metropolis algorithm [30], which was originally proposed to find the equilibrium configuration of a collection of atoms. The great advantage of SA is its ability to move uphill with a probability given by a Boltzmann distribution. The possibility of uphill moves prevents SA from becoming stuck at local minima. SA has been used by a wide and highly interdisciplinary community. It has been applied, for instance, to chemical and biological problems like conformational optimizations on potential energy surfaces [31–33], or in studies modelling proteins [34,35], among others.

In this work, we develop a general approach to minimize specific elements of the rovibrational \mathbf{G} matrix, considered as a function of the Euler angles, in molecules of arbitrary complexity and size. The goal is to obtain the optimal orientation of the molecule-fixed axes that minimizes rovibrational or pure rotational terms. In this form, the optimal (or at least suboptimal) form of the rovibrational Hamiltonian can be obtained. To such an end, a metaheuristic approach based in SA is developed, calibrated and tested using a set of non-rigid molecules.

2. Methodology

In this section we present the theoretical and algorithmic components of the treatment proposed.

2.1. Rovibrational Hamiltonian

As shown by Meyer and Günthard [6], and Pickett [7] a general rovibrational Hamiltonian in arbitrary curvilinear internal coordinates can be obtained as:

$$\hat{H} = -\frac{\hbar^2}{2} \sum_{i=1}^{3N-3} \sum_{j=1}^{3N-3} \left[g_{ij} \frac{\partial^2}{\partial q_i \partial q_j} + \left(\frac{\partial g_{ij}}{\partial q_i} \right) \frac{\partial}{\partial q_j} \right] + V(q_3, \dots, q_{3N-3}) \quad (1)$$

where the first term is the kinetic part and the **second one** is the potential function. The g_{ij} are the elements of the rovibrational \mathbf{G} matrix [7,8,36]. Both terms in Eq. (1) depend on a suitable set of vibrational coordinates, \mathbf{q} .

The kinetic operator in Eq. (1) can be expressed more compactly in terms of the conjugate momenta with respect to the overall rotation, \mathbf{J} , and with respect to the change on the vibrational coordinates, \mathbf{p} , as [37]:

$$\hat{T} = -\frac{\hbar^2}{2} (\hat{\mathbf{J}} \mathbf{G}_R \hat{\mathbf{J}} + \hat{\mathbf{J}} \mathbf{G}_{RV} \hat{\mathbf{p}} + \hat{\mathbf{p}} \mathbf{G}_{RV}^T \hat{\mathbf{J}} + \hat{\mathbf{p}} \mathbf{G}_V \hat{\mathbf{p}}) \quad (2)$$

\mathbf{G}_R , \mathbf{G}_V and \mathbf{G}_{RV} are block components of the rovibrational \mathbf{G} matrix defined as [8]:

$$\mathbf{G} = \begin{pmatrix} \mathbf{G}_R & \mathbf{G}_{RV} \\ \mathbf{G}_{RV}^T & \mathbf{G}_V \end{pmatrix} = \begin{pmatrix} \mathbf{I} & \mathbf{X} \\ \mathbf{X}^T & \mathbf{Y} \end{pmatrix}^{-1} \quad (3)$$

Here, \mathbf{G}_R and \mathbf{G}_V are pure rotational and pure vibrational submatrices, respectively. \mathbf{G}_{RV} is the rotational–vibrational coupling submatrix. As shown in Eq. (3), to get \mathbf{G}_R , \mathbf{G}_V , and \mathbf{G}_{RV} we need the inertial tensor, \mathbf{I} , the pure vibrational \mathbf{Y} matrix, and the \mathbf{X} matrix representing the vibration–rotation interaction (Coriolis terms). The elements of \mathbf{I} , \mathbf{X} and \mathbf{Y} are obtained from the molecular structure [7,8,36].

The \mathbf{G} matrix can be considered as the blockwise inverse of a block matrix in terms of its blocks (here, the \mathbf{I} , \mathbf{X} and \mathbf{Y} matrices) [38]. Therefore,

$$\mathbf{G} = \begin{pmatrix} \mathbf{G}_R & \mathbf{G}_{RV} \\ \mathbf{G}_{RV}^T & \mathbf{G}_V \end{pmatrix} = \begin{pmatrix} \mathbf{I}^{-1} + \mathbf{I}^{-1}\mathbf{X}(\mathbf{Y} - \mathbf{X}^T\mathbf{I}^{-1}\mathbf{X})^{-1}\mathbf{X}^T\mathbf{I}^{-1} & -\mathbf{I}^{-1}\mathbf{X}(\mathbf{Y} - \mathbf{X}^T\mathbf{I}^{-1}\mathbf{X})^{-1} \\ -(\mathbf{Y} - \mathbf{X}^T\mathbf{I}^{-1}\mathbf{X})^{-1}\mathbf{X}^T\mathbf{I}^{-1} & (\mathbf{Y} - \mathbf{X}^T\mathbf{I}^{-1}\mathbf{X})^{-1} \end{pmatrix} \quad (4)$$

Eq. (4) shows that the \mathbf{G} matrix submatrices depend on the Schur complement of the inertial tensor \mathbf{I} : $\mathbf{Y} - \mathbf{X}^T\mathbf{I}^{-1}\mathbf{X}$. In particular, the \mathbf{G}_V submatrix is given by the inverse of this factor.

It is important to realize that the rovibrational Hamiltonian, Eq. (1), depends on the elements of the \mathbf{G} matrix. Thus, it is not strictly correct to discuss rotation and vibration in terms of the \mathbf{I} , \mathbf{X} and \mathbf{Y} matrices, since a matrix inversion is involved and the original elements are in more or less extend mixed, see Eq. (4). Only when the rotation–vibration coupling is zero we have $\mathbf{X} = \mathbf{0}$, and the \mathbf{G} matrix elements are directly given by $\mathbf{G}_R = \mathbf{I}^{-1}$ and $\mathbf{G}_V = \mathbf{Y}^{-1}$.

In the general case, the \mathbf{G} matrix depends on the vibrational coordinates. Thus, it is necessary to consider this dependence. The usual treatment dates back at least twenty-seven years, see Ref. [39]. The key point is to generate different molecular structures corresponding to different displacements from the equilibrium position along the vibrational coordinates. For each of these structures we determine the \mathbf{G} matrix in the same molecule-fixed reference frame. Useful functional forms for the \mathbf{G} matrix elements are generated by using Taylor expansions for non-periodic vibrations and Fourier series for periodic ones, see Refs. [40–47]. The functional forms are obtained by fitting the g_{ij} elements to the Taylor/Fourier expansions on the vibrational coordinates.

2.2. Effect of the rotation of axes

The rotation of the space-fixed axes to obtain the desired molecule-fixed can be described through a rotation matrix, \mathbf{A} . Using the Euler angles (θ, ϕ, ψ) , describing the orientation in space of the molecule-fixed axes, \mathbf{A} can be obtained as [5]:

$$\mathbf{A} = \begin{pmatrix} \cos \psi \cos \phi - \cos \theta \sin \phi \sin \psi & -\cos \psi \sin \phi + \cos \theta \cos \phi \sin \psi & \sin \psi \sin \theta \\ -\sin \psi \cos \phi - \cos \theta \sin \phi \cos \psi & -\sin \psi \sin \phi + \cos \theta \cos \phi \cos \psi & \cos \psi \sin \theta \\ \sin \theta \sin \phi & -\sin \theta \cos \phi & \cos \theta \end{pmatrix} \quad (5)$$

Knowing \mathbf{A} , we can determine the effect of a rotation of axes in the rovibrational Hamiltonian. Therefore, we need to consider the effect of \mathbf{A} on the \mathbf{I} , \mathbf{X} and \mathbf{Y} matrices in Eq. (4).

The \mathbf{A} matrix acts on the nuclear coordinates, \mathbf{r} , generating a new coordinates set $\mathbf{r}' = \mathbf{A} \cdot \mathbf{r}$.

Therefore,

$$\mathbf{I}' = \mathbf{A} \cdot \mathbf{I} \cdot \mathbf{A}^T, \quad \mathbf{X}' = \mathbf{A} \cdot \mathbf{X} \quad (6)$$

In turn, upon rotation of coordinates, the derivatives are also rotated, $\mathbf{D}' = \mathbf{A} \cdot \mathbf{D}$. However, the \mathbf{Y} matrix is related to the product $\mathbf{D}^T \cdot \mathbf{D}$ that equals $\mathbf{D}'^T \cdot \mathbf{D}'$, because of the orthogonality of \mathbf{A} . In other words, the \mathbf{Y} matrix is independent of the rotation of the axes.

Using Eqs. (4) and (6) we can determine the effect of rotation on the rovibrational \mathbf{G} matrix. It is convenient to start with the Schur complement of \mathbf{I}' , which is transformed as,

$$\mathbf{Y}' - \mathbf{X}'^T\mathbf{I}'^{-1}\mathbf{X}' = \mathbf{Y} - (\mathbf{X}^T\mathbf{A}^T)(\mathbf{A}\mathbf{I}^{-1}\mathbf{A}^T)(\mathbf{A}\mathbf{X}) = \mathbf{Y} - \mathbf{X}^T\mathbf{I}^{-1}\mathbf{X} \quad (7)$$

Eqs. (4) and (7) show that the \mathbf{G}_V submatrix is invariant upon rotation of axes. In turn, substituting Eqs. (6) and (7) in Eq. (4) we get that the pure rotational \mathbf{G}_R , and rovibrational \mathbf{G}_{RV} submatrices are transformed as

$$\mathbf{G}'_R = \mathbf{A} \cdot \mathbf{G}_R \cdot \mathbf{A}^T, \quad \mathbf{G}'_{RV} = \mathbf{A} \cdot \mathbf{G}_{RV} \quad (8)$$

Thus, once an initial \mathbf{G} matrix is known, the corresponding \mathbf{G}' matrix in a new set of rotating coordinates can be obtained by computing the \mathbf{A} matrix, see Eq. (5). Clearly, the \mathbf{A} matrix elements take different values for each choice of the three Euler angles (θ, ϕ, ψ) .

2.3. Selection of optimal molecule-fixed axes orientation

The treatment we propose to choose the optimal orientation of molecule-fixed axes minimizes a cost function, $f(\theta, \phi, \psi)$, composed by selected elements of the \mathbf{G} matrix. These elements are considered as a function of the three Euler angles. Thus,

$$f(\theta, \phi, \psi) = \sum_{ij} |g_{ij}(\theta, \phi, \psi)| \quad (9)$$

The goal is to obtain the \mathbf{G} matrix corresponding to the Euler angles providing the global minimum of $f(\theta, \phi, \psi)$.

In the present study we select three cases. The first corresponds to the minimization of the non-diagonal elements of the pure rotational \mathbf{G}_R submatrix. In the second, we minimize the rovibrational interaction (Coriolis) term, \mathbf{G}_{RV} . Finally, the third corresponds to the minimization of the \mathbf{G}_{RV} term plus the non-diagonal terms of the \mathbf{G}_R submatrix. Note that, as shown by Eq. (4), the first case is not equivalent to reduce \mathbf{I} to diagonal form (principal axes of inertia). Accordingly, the second case is not equivalent to minimizing the \mathbf{X} matrix (Eckart or Eckart-like axes). The search, or definition, space is given by the Euler angles values range: $0 \leq \theta \leq \pi$, $0 \leq \phi \leq 2\pi$, and $0 \leq \psi \leq 2\pi$.

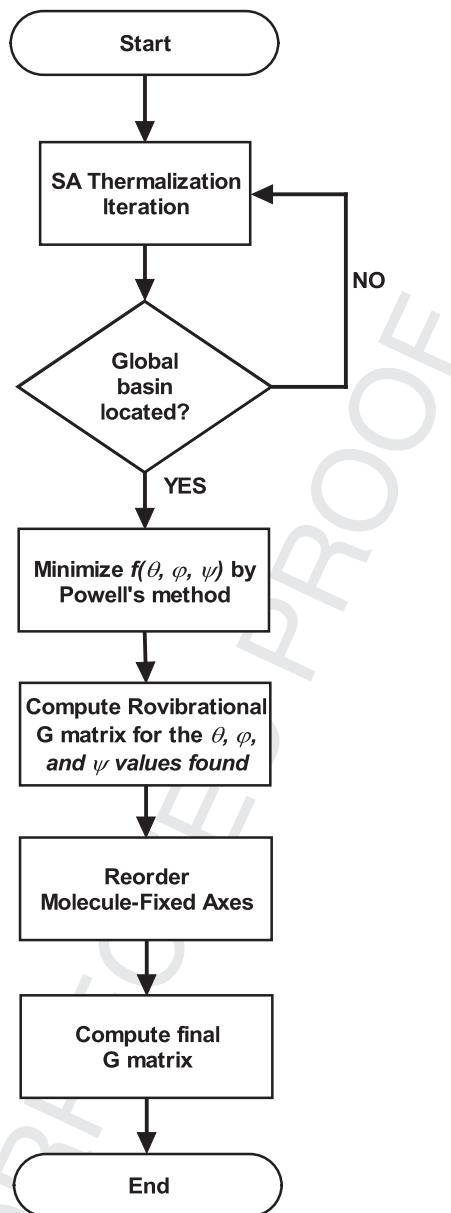


Fig. 1. Flowchart showing the functional model of the molecule-fixed axes selection algorithm.

2.4. Minimization of the cost function

Location of the global minimum of the $f(\theta, \phi, \psi)$ cost function can be tackled by simulated annealing (SA). SA is an iterative process, see Refs. [27,28]. In each step we consider the current state of $f(\theta, \phi, \psi)$, given by the value of the Euler angles. Then, we probabilistically decide if the current state is changed to a new one or if the initial state remains. The decision is made applying the Metropolis condition [30], which uses a Boltzmann probability distribution: $\exp[-f(\theta, \phi, \psi)/T]$. In this approach, the “temperature” T is a parameter initially fixed to a high value of the f cost function. This process is repeated until the system “thermalizes”, i.e., it reaches a steady state or is close enough to it. Then the procedure is repeated for decreasing values of the “temperature” (freezing). Along this procedure, the function f explores all its definition space using random displacements, which define a Markov chain. As the temperature goes down, the function localizes around the global minimum. The procedure stops when we reach a temperature low enough, or a sufficiently small value of the cost function.

Finding the global, or an enough low local, minimum by SA can result in a large number of cost function evaluations. However, it is important to realize that a global optimization method is only needed for locating the basin of the global minimum. After that, we can resort to local optimization techniques, which are more economical in terms of cost function evaluations. To prevent the computation of cost function gradients, we select here a function-based method. In particular we select the Powell’s optimization method [48]. Powell’s method is a multidimensional direction set method of local minimization. It works maintaining a set of independent directions u_1, u_2, \dots, u_n , performing successive line searches along the u_i ’s in a cyclical manner [49]. Combining SA with Powell’s method we obtain a multidimensional global optimization method that keeps under control the number of cost function evaluations. Fig. 1 shows schematically the logic of the proposed SA + Powell global optimization procedure.

Start

α : Initial parameter. Maximum variation allowed for the θ , ϕ , and ψ angles
 β : Initial parameter. Per cent increment determining the starting temperature

Compute θ , ϕ and ψ randomly

Compute $f_0(\theta, \phi, \psi)$

for $i=1$ **to** 100 : Making an inexpensive survey of the definition space

 Compute θ , ϕ and ψ randomly

 Compute $f(\theta, \phi, \psi)$

if $f_0 < f$ **then**

$f_0 = f$

end_if

end_for

$T = (1 + \beta) * f_0$: Selecting initial temperature (β % higher than the maximum f located)

repeat : Freezing cycles

for $i=1$ **to** Niter: Niter is the number of iterations to achieve thermalization

 /* Generating Markov chain of states */

$\theta = \theta + \alpha * \text{random}(0, 1)$

$\phi = \phi + \alpha * \text{random}(0, 1)$

$\psi = \psi + \alpha * \text{random}(0, 1)$

 /* Allowing to explore the full range of Euler angles */

if $\theta > \pi$ **then** $\theta = \theta - \pi$

if $\phi > 2\pi$ **then** $\phi = \phi - 2\pi$

if $\psi > 2\pi$ **then** $\psi = \psi - 2\pi$

 Compute $f_1(\theta, \phi, \psi)$

 /* Applying Metropolis algorithm */

if $f_1 < f_0$ **then**

$f_0 = f_1$

else

$\delta = f_1 - f_0$

if $\exp(-\delta/T) > \text{random}(0,1)$ **then**

$f_0 = f_1$

end_if

end_if

end_for

$T = g(T)$: g is a decreasing function such as $T_{i+1} < T_i$

until Stop Criteria

return last (optimal) θ , ϕ , and ψ values

End

Fig. 2. Pseudocode for the SA procedure.

3. Results and discussion

3.1. Calibration of the treatment

Using the previous molecular set and the defined torsional vibrational coordinates, we determine the different parameters in the SA method described above. The three chosen cost functions are defined as,

$$f(\mathbf{G}_R) = \sum_{i=1}^3 \sum_{j=i+1}^3 |g_{ij}(\theta, \phi, \psi)| \quad \text{case a)}$$

$$f(\mathbf{G}_{RV}) = \sum_{i=1}^3 \sum_{j=3+i}^{3N-3} |g_{ij}(\theta, \phi, \psi)| \quad \text{case b)}$$

$$f(\mathbf{G}_R + \mathbf{G}_{RV}) = \sum_{i=1}^3 \sum_{j=i+1}^3 |g_{ij}(\theta, \phi, \psi)| + \sum_{i=1}^3 \sum_{j=3+i}^{3N-3} |g_{ij}(\theta, \phi, \psi)| \quad \text{case c)} \quad (12)$$

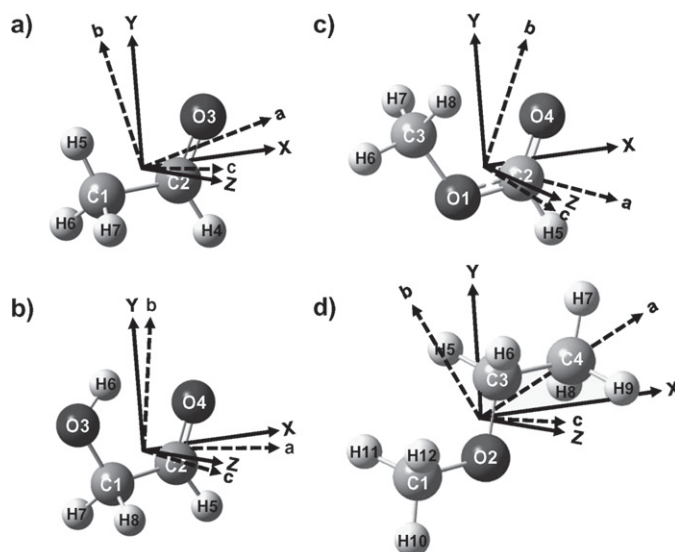


Fig. 3. Molecular structure and numbering convention for the molecular set used in this work. a) Acetaldehyde, b) Glycolaldehyde, c) Methyl formate, and d) Ethyl methyl ether. The solid axes are the space-fixed axes. In all cases, the XY -plane contains the heavy atoms of the molecules. The dotted axes represent the molecule-fixed axes, as described in the text in Section 3.2.

Case a) corresponds to the minimization of the pure rotational non-diagonal terms in the 3×3 submatrix \mathbf{G}_R . Case b) is used to minimize the rotation-vibration interaction submatrix \mathbf{G}_{RV} . Finally, case c) combines the a) and b) cases. Given the previous cases definitions, we use the average cost function, $\langle f \rangle$, as an index to determine the value of the parameters to be used in our SA algorithm. Using a probabilistic acceptance criterion, as the Metropolis condition, it is possible to prove [28] that the $\langle f \rangle$ value is simply the average of the computed f ,

$$\langle f \rangle \approx \sum_{i=1}^N f_i / N \quad (13)$$

This approximation becomes exact as N goes to infinity.

The first parameter to determine is the maximum displacement, α , allowed for a random variation of the Euler angles. Thus, we perform several tests for a fixed temperature; see Fig. 4, using α values of 10° and 20° . The same α is used for the three Euler angles. Enough configurations (1000) are generated, see inner loop in Fig. 2, to achieve thermalization. Thermalization is monitored through the variation of the average value of the cost function, $\langle f(\theta, \phi, \psi) \rangle$. As cost function we select the case c) (the most general) in Eq. (12). The working temperature is determined using an initial scan of 100 randomly determined values of the $f(\theta, \phi, \psi)$ function. The temperature is chosen as the medium point between the maximum and minimum $f(\theta, \phi, \psi)$ values found. Fig. 4 shows the results obtained for the set of calibration molecules. Here, we observe that thermalization is obtained for about 400 configurations. We consider this value as a conservative approach, and we select it as the number of configurations, length of the Markov chain, to generate for each temperature. Thus, the Niter variable in the pseudocode of Fig. 2 is set to 400. In addition, Fig. 4 shows that α values of 10° and 20° yield quite similar results. Thus, we select $\alpha = 20^\circ$, since this leads to a faster exploration of the θ , ϕ , and ψ definition space.

For the SA procedure to work properly, the initial temperature must be greater than the maximum value of the cost function [27-29]. Here, we set the initial temperature to a given proportion of the maximum cost function value found in the initial 100 random values scan. We consider increments over this value of 200%, 300%, 400% and 30%. As cost function we use the case c) of Eq. (12). The temperature decreasing function, $g(T)$ in Fig. 2, is selected by imposing an exponential decreasing form, such that $T_{i+1} = r * T_i$. As freezing factor, r , we have selected arbitrarily a 0.90 value, in consonance with the recommendations found in the literature [27,28]. The four molecules of the calibration set, in its equilibrium position, are used. In all cases, we find that the same minimum, for each molecule, is obtained using any of the increments for the initial temperature. Since the number of iterations in the freezing process, outer loop in Fig. 2, depends on this starting point, we select the smallest, 30%, increment. In this form, we reduce the number of iterations.

The last point to consider is when to start the Powell's local optimization, see Fig. 1. The basic idea is to determine when the SA has reached the global minimum basin. Then, we shut down SA and start the Powell's minimization method. We determine SA is in the basin of the global minimum when the f value is close enough to this minimum. Fig. 5 shows the evolution of the f value for the case c) of Eq. (12) in the four calibration molecules, as a function of the number of decreasing temperatures, n_t . We observe that in all cases an n_t between 40 to 80 places the cost function close to its minimum value. We have found that applying the following heuristic, we can identify when we are in this region of the cost function. First, we require the difference between the two last values of the $f(\theta, \phi, \psi)$ function to be smaller than 1.0×10^{-4} ($\text{amu}\text{\AA}^2$) $^{-1}$. Second, we require that this situation would be repeated at least four successive times. The dotted vertical line in Fig. 5 shows, for each molecule, the point where the local Powell's minimization starts using the previous heuristic. In all the tests performed, starting Powell's method in these conditions leads to the same minima (in fact to a smaller value) that a SA procedure repeated a total of $n_t = 200$ times, see Fig. 5. In addition, the computational cost, measured as number of $f(\theta, \phi, \psi)$ evaluations, is much smaller.

3.2. Analysis of results and conclusions

The previous minimizing technique has been applied to the computation of the \mathbf{G} matrix for the four molecules in the calibration set. In all cases, the periodic torsional coordinates defined in Section 2.4 are used as vibrational coordinates.

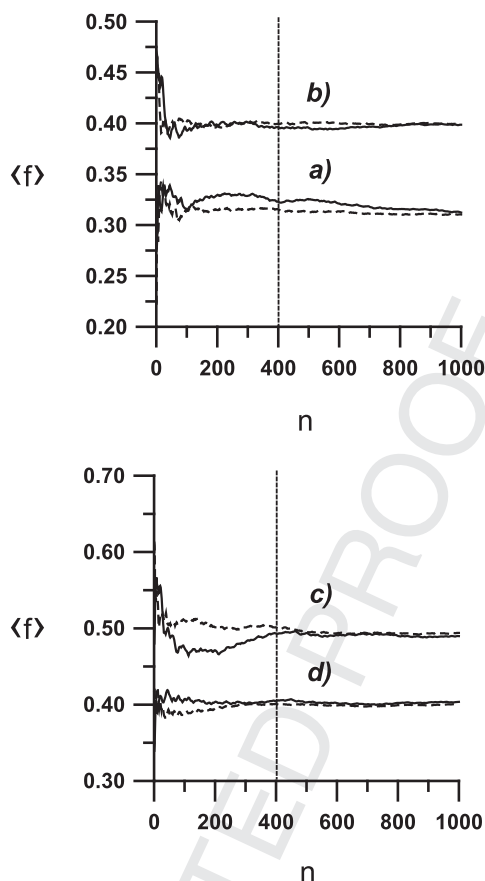


Fig. 4. Average cost function, $\langle f \rangle$, in $(\text{amu}\text{\AA}^2)^{-1}$, as a function of the number of thermalization iterations, n . a) Acetaldehyde, b) Glycolaldehyde, c) Methyl formate, and d) Ethyl methyl ether. Data obtained from the equilibrium structures determined at the MP2/cc-pVQZ level of theory. Continuous line, $\alpha = 10$ degrees. Dashed line, $\alpha = 20$ degrees.

In all cases, we have used the minimum energy conformations. For the sake of comparison, we have considered four different cases corresponding to different orientations of the molecule-fixed axes. The first case corresponds to the principal axes of inertia. The results are the ones provided by the Gmat program in its present, 1.0, version [51]. This case corresponds formally to the minimization of the non-diagonal terms in the inertial tensor, \mathbf{I} . The cost function here can be symbolized as $f(\mathbf{I})$. The three remaining cases correspond to the cases in Eq. (12). The results are collected in Tables 1 and 2. We observe in the four molecules that, as stated in Eq. (7), the pure vibrational \mathbf{G}_V elements remain constant. This justifies the use of pure vibrational Hamiltonians in the study of large-amplitude vibrations; see for instance Refs. [41,44–47] and [52,53], using any molecule-fixed axes orientation.

With respect to the results using principal axes of inertia, $f(\mathbf{I})$ case, we observe that despite the \mathbf{I} tensor is diagonal, the pure rotational \mathbf{G}_R submatrix is not. This is a consequence of the term added to \mathbf{I}^{-1} in \mathbf{G}_R , see Eq. (4). Therefore, the principal axes of inertia are not the most appropriate to simplify the pure rotational contribution to the rovibrational Hamiltonian. In contrast, Tables 1 and 2 show that minimizing the $f(\mathbf{G}_R)$ cost function is the way to diagonalize the pure rotational \mathbf{G}_R submatrix.

Considering the rotation–vibration submatrix, \mathbf{G}_{RV} , Tables 1 and 2 show that even when minimized, $f(\mathbf{G}_{RV})$ case, some of its elements keep a large value compared with the \mathbf{G}_R ones. However, the vibration modes here considered are torsional, and it would be expected an important coupling of these modes with overall rotation. The situation could differ for bending or stretching modes. Anyway, the present methodology makes easy to analyze this problem in any molecule.

Finally, we observe that the $f(\mathbf{G}_R + \mathbf{G}_{RV})$ case does not achieve in all cases full diagonalization of the \mathbf{G}_R submatrix. In addition, the \mathbf{G}_{RV} elements keep values similar to those obtained in the $f(\mathbf{G}_{RV})$ case.

These results suggest that any rotational–vibrational treatment would need to handle at least some \mathbf{G}_{RV} elements, as long as rotational levels are needed. Being able to handle \mathbf{G}_{RV} elements, the most appropriate molecule-fixed axes orientation is the one that minimizes the $f(\mathbf{G}_R)$ cost function, since it leads to the simplest expression for the pure rotational contribution.

The present treatment makes it easy to identify the molecule-fixed axes defining the most important rovibrational coupling terms. To such an end, we have included in Fig. 3 the a , b , and c molecule-fixed axes. The figure depicts the axes orientation for the $f(\mathbf{G}_R + \mathbf{G}_{RV})$ case. However, qualitatively the orientation is similar, in all molecules, for the remaining three cases. We observe in Tables 1 and 2 that the largest rovibrational coupling terms, \mathbf{G}_{RV} elements, for each molecule are the same in the four cases considered. For acetaldehyde, Table 1 shows the largest coupling corresponding to the coupling between the rotation on the a axis and the methyl torsion, $g_{0,3}$ element. This is the expected behaviour since Fig. 3 shows that the a -axis is nearly parallel to the methyl rotation axis. The results are similar in the remaining molecules. In all cases, we observe that the torsional degrees of freedom are more strongly coupled with the a - and b -axes. Fig. 3 shows that in the four molecules the ab -plane is close to the XY -plane. In turn, the XY -plane contains the heavy atoms. Thus, the ab -plane should approximately contain the torsional axes of the considered torsional vibrations. As in the acetaldehyde case, this explains

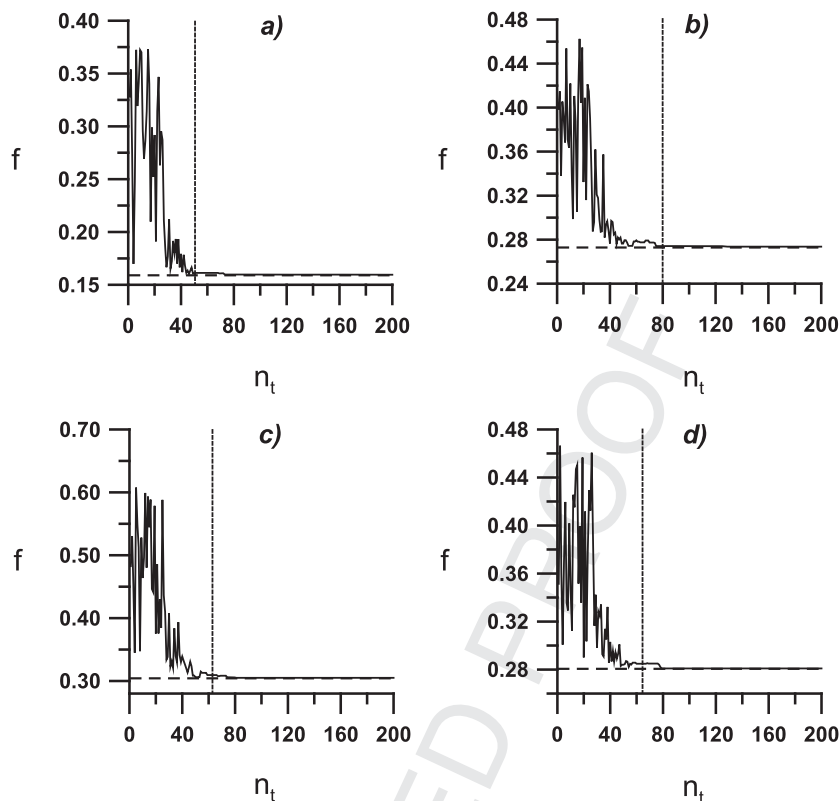


Fig. 5. Cost function value, f , in $(\text{amu}\text{\AA}^2)^{-1}$, as a function of the number of temperatures of the SA process, n_t . a) Acetaldehyde, b) Glycolaldehyde, c) Methyl formate, and d) Ethyl methyl ether. Data obtained from the equilibrium structures determined at the MP2/cc-pVQZ level of theory.

Table 1

G matrix elements, in cm^{-1} , of Acetaldehyde and Glycolaldehyde after selection of the molecule-fixed axes orientation. Data obtained from the equilibrium structures determined at the MP2/cc-pVQZ level of theory. The torsional coordinates defined in Section 2.4 are used as vibration coordinates. $f(\mathbf{I})$ corresponds to the principal axes of inertia. $f(\mathbf{G}_R)$ minimizes the non-diagonal elements of the 3×3 \mathbf{G}_R submatrix. $f(\mathbf{G}_{RV})$ minimizes the rotation-vibration coupling. Finally, $f(\mathbf{G}_R + \mathbf{G}_{RV})$ is the combination of the two previous cases.

		Acetaldehyde			
		$f(\mathbf{I})$	$f(\mathbf{G}_R)$	$f(\mathbf{G}_{RV})$	$f(\mathbf{G}_R + \mathbf{G}_{RV})$
\mathbf{G}_R	$\mathbf{g}_{0,0}$	2.746815	2.748728	2.742083	2.742083
	$\mathbf{g}_{1,1}$	0.345812	0.343899	0.350544	0.350544
	$\mathbf{g}_{2,2}$	0.304990	0.304990	0.304990	0.304990
	$\mathbf{g}_{0,1}$	-0.067799	0.000	0.126241	0.126241
	$\mathbf{g}_{0,2}$	-3.000e-12	0.000	-4.390e-10	-1.050e-10
	$\mathbf{g}_{1,2}$	3.000e-12	3.000e-12	-1.950e-10	-5.000e-12
\mathbf{G}_{RV}	$\mathbf{g}_{0,3}$	-2.546199	-2.551002	-2.554534	-2.554534
	$\mathbf{g}_{1,3}$	0.206180	0.134285	-3.000e-11	6.685e-08
	$\mathbf{g}_{2,3}$	5.000e-12	1.000e-12	-1.320e-10	1.020e-10
	$\mathbf{g}_{3,3}$	7.743128	7.743128	7.743128	7.743128
		Glycolaldehyde			
		$f(\mathbf{I})$	$f(\mathbf{G}_R)$	$f(\mathbf{G}_{RV})$	$f(\mathbf{G}_R + \mathbf{G}_{RV})$
\mathbf{G}_R	$\mathbf{g}_{0,0}$	1.341392	1.533479	1.510759	1.533479
	$\mathbf{g}_{1,1}$	0.514945	0.322858	0.345578	0.322858
	$\mathbf{g}_{2,2}$	0.167957	0.167957	0.167957	0.167957
	$\mathbf{g}_{0,1}$	-0.442320	0.000	-0.164284	0.000
	$\mathbf{g}_{0,2}$	8.526e-06	0.000	3.347e-05	4.463e-06
	$\mathbf{g}_{1,2}$	-7.351e-06	-1.471e-05	-8.170e-06	4.507e-06
\mathbf{G}_{RV}	$\mathbf{g}_{0,3}$	1.687875	1.985689	1.921061	1.985689
	$\mathbf{g}_{1,3}$	-1.098330	-0.335099	-0.603967	-0.335099
	$\mathbf{g}_{2,3}$	2.613e-05	3.509e-05	6.069e-05	2.539e-09
	$\mathbf{g}_{0,4}$	-1.946946	-2.002352	-2.021410	-2.002352
	$\mathbf{g}_{1,4}$	0.543597	-0.276920	2.277e-09	-0.276920
	$\mathbf{g}_{2,4}$	3.512e-05	7.121e-05	9.198e-07	3.030e-07
\mathbf{G}_V	$\mathbf{g}_{3,3}$	4.128962	4.128962	4.128962	4.128962
	$\mathbf{g}_{3,4}$	-2.646526	-2.646526	-2.646526	-2.646526
	$\mathbf{g}_{4,4}$	22.514102	22.514102	22.514102	22.514102

Table 2
G matrix elements, in cm^{-1} , of Methyl formate and Ethyl methyl ether after selection of the molecule-fixed axes orientation. Data obtained from the equilibrium structures determined at the MP2/cc-pVQZ level of theory. The torsional coordinates defined in Section 2.4 are used as vibration coordinates. $f(\mathbf{I})$ corresponds to the principal axes of inertia. $f(\mathbf{G}_R)$ minimizes the non-diagonal elements of the 3×3 \mathbf{G}_R submatrix. $f(\mathbf{G}_{RV})$ minimizes the rotation–vibration coupling. Finally, $f(\mathbf{G}_R + \mathbf{G}_{RV})$ is the combination of the two previous cases.

		Methyl formate			
		$f(\mathbf{I})$	$f(\mathbf{G}_R)$	$f(\mathbf{G}_{RV})$	$f(\mathbf{G}_R + \mathbf{G}_{RV})$
\mathbf{G}_R	$\mathbf{g}_{0,0}$	1.826902	2.187276	2.166093	2.171070
	$\mathbf{g}_{1,1}$	0.696604	0.336230	0.357413	0.352436
	$\mathbf{g}_{2,2}$	0.178888	0.178888	0.178888	0.178888
	$\mathbf{g}_{0,1}$	-0.732938	0.000	0.196877	0.172436
	$\mathbf{g}_{0,2}$	2.389e-05	0.000	-9.620e-06	-1.169e-05
\mathbf{G}_{RV}	$\mathbf{g}_{1,2}$	-1.504e-05	-3.333e-06	-6.831e-06	-8.439e-06
	$\mathbf{g}_{0,3}$	2.561697	3.014046	3.031442	3.031166
	$\mathbf{g}_{1,3}$	-1.620908	-0.324286	-3.071e-08	-0.040848
	$\mathbf{g}_{2,3}$	5.181e-05	1.044e-05	-1.818e-09	-2.080e-08
	$\mathbf{g}_{0,4}$	-1.605088	-1.875265	-1.883357	-1.883528
\mathbf{G}_V	$\mathbf{g}_{1,4}$	0.985581	0.176235	-0.025380	-6.356e-09
	$\mathbf{g}_{2,4}$	-3.834e-05	-1.254e-05	-5.656e-06	-5.393e-06
	$\mathbf{g}_{3,3}$	5.779891	5.779891	5.779891	5.779891
	$\mathbf{g}_{3,4}$	-2.750706	-2.750706	-2.750706	-2.750706
	$\mathbf{g}_{4,4}$	6.995153	6.995153	6.995153	6.995153
		Ethyl methyl ether			
		$f(\mathbf{I})$	$f(\mathbf{G}_R)$	$f(\mathbf{G}_{RV})$	$f(\mathbf{G}_R + \mathbf{G}_{RV})$
\mathbf{G}_R	$\mathbf{g}_{0,0}$	1.823615	1.894117	1.870489	1.870489
	$\mathbf{g}_{1,1}$	0.398219	0.327718	0.351346	0.351346
	$\mathbf{g}_{2,2}$	0.131297	0.131297	0.131297	0.131297
	$\mathbf{g}_{0,1}$	0.324750	0.000	0.190925	0.190925
	$\mathbf{g}_{0,2}$	1.325e-06	0.000	-1.161e-06	-3.144e-07
\mathbf{G}_{RV}	$\mathbf{g}_{1,2}$	3.899e-07	2.312e-07	1.045e-07	-6.069e-08
	$\mathbf{g}_{0,3}$	0.941665	1.065349	0.999720	0.999720
	$\mathbf{g}_{1,3}$	0.684036	0.468688	0.595984	0.595983
	$\mathbf{g}_{2,3}$	1.171e-06	6.522e-07	-2.170e-10	-1.439e-07
	$\mathbf{g}_{0,4}$	1.187713	1.138754	1.173482	1.173482
\mathbf{G}_V	$\mathbf{g}_{1,4}$	-0.103334	-0.352958	-0.210426	-0.210426
	$\mathbf{g}_{2,4}$	8.790e-07	-2.474e-07	-1.011e-06	5.160e-10
	$\mathbf{g}_{0,5}$	-1.553688	-1.548282	-1.560093	-1.560093
	$\mathbf{g}_{1,5}$	-0.141226	0.191607	4.867e-09	2.031e-09
	$\mathbf{g}_{2,5}$	-3.923e-06	-2.584e-06	-1.568e-06	-2.550e-06
\mathbf{G}_V	$\mathbf{g}_{3,3}$	1.829018	1.829018	1.829018	1.829018
	$\mathbf{g}_{3,4}$	-0.040559	-0.040559	-0.040559	-0.040559
	$\mathbf{g}_{3,5}$	-0.598811	-0.598811	-0.598811	-0.598811
	$\mathbf{g}_{4,4}$	6.486525	6.486525	6.486525	6.486525
	$\mathbf{g}_{4,5}$	-1.136572	-1.136572	-1.136572	-1.136572
	$\mathbf{g}_{5,5}$	6.692732	6.692732	6.692732	6.692732

the larger rovibrational coupling respect to these axes. Clearly, the ζ -axis, being almost perpendicular to the torsional axes, exhibits the smaller rovibrational coupling.

Acknowledgements

This work has been cofinanced by FEDER funds and the Consejería de Educación y Ciencia de la Junta de Comunidades de Castilla-La Mancha (grant # PBI08-0008). The Ministerio de Educación y Ciencia (grant # AYA 2008-00446) is also acknowledged. M.E. Castro thanks the Consejo Nacional de Ciencia y Tecnología, CONACyT (Mexico) for a graduate grant (grant # 171982), and the Ministerio de Asuntos Exteriores y de Cooperación-Agencia Española de Cooperación Internacional para el Desarrollo, MAEC-AECID.

References

- [1] E.B. Wilson Jr., J.C. Decius, C. Cross, Molecular Vibrations, Dover, New York, 1980.
- [2] D. Papousek, M.R. Aliev, Molecular Vibrational/Rotational Spectra, Academia, Prague, 1982.
- [3] P.R. Bunker, P. Jensen, Molecular Symmetry and Spectroscopy, second edition, NRC-Research Press, Ottawa, 1998.
- [4] S. Califano, Vibrational States, Wiley, London, 1976.
- [5] H. Goldstein, Classical Mechanics, second edition, Addison-Wesley Publishing Company, USA, 1980.
- [6] R. Meyer, Hs.H. Günthard, J. Chem. Phys. 49 (1968) 1510.
- [7] H.M. Pickett, J. Chem. Phys. 56 (1972) 1715.
- [8] M.A. Harthcock, J. Laane, J. Chem. Phys. 89 (1985) 4231.
- [9] H.B.G. Casimir, Rotation of a Rigid Body in Quantum Mechanics, J.B. Wolters, Den Haag, 1931.
- [10] C. Eckart, Phys. Rev. 47 (1935) 552.
- [11] E.B. Wilson Jr., J.B. Howard, J. Chem. Phys. 4 (1936) 260.
- [12] B.T. Darling, D.M. Dennison, Phys. Rev. 57 (1940) 128.

- 1 [13] J.K.G. Watson, *Mol. Phys.* 15 (1968) 479. 1
- 2 [14] J.K.G. Watson, *Mol. Phys.* 19 (1970) 465. 2
- 3 [15] K.N. Kudin, A.Y. Dymarsky, *J. Chem. Phys.* 122 (2005) 224105. 3
- 4 [16] D. Janezic, M. Praprotnik, *Int. J. Quant. Chem.* 84 (2001) 2. 4
- 5 [17] D. Janezic, M. Praprotnik, F. Merzel, *J. Chem. Phys.* 122 (2005) 174101. 5
- 6 [18] M. Praprotnik, D. Janezic, *J. Chem. Phys.* 122 (2005) 174102. 6
- 7 [19] M. Praprotnik, D. Janezic, *J. Chem. Phys.* 122 (2005) 174103. 7
- 8 [20] M. Praprotnik, D. Janezic, *J. Chem. Inf. Model* 45 (2005) 1571. 8
- 9 [21] J. Tennyson, Variational calculations of rotation-vibration spectra, in: P. Jensen, P.R. Bunker (Eds.), *Computational Molecular Spectroscopy*, John Wiley & Sons, UK, 2000, 9
- 10 p. 305. 10
- 11 [22] J.T. Hougen, P.R. Bunker, J.W.C. Johns, *J. Mol. Spectrosc.* 34 (1970) 136. 11
- 12 [23] B.T. Sutcliffe, J. Tennyson, *Int. J. Quant. Chem.* 39 (1991) 183. 12
- 13 [24] H. Wei, T. Carrington Jr., *J. Chem. Phys.* 107 (1997) 2813. 13
- 14 [25] H. Wei, T. Carrington Jr., *J. Chem. Phys.* 107 (1997) 9493. 14
- 15 [26] J. Makarewicz, A. Bauder, *Mol. Phys.* 84 (1995) 853. 15
- 16 [27] J. Dréo, P. Siarry, A. Pétrowski, E. Taillard, *Metaheuristics for Hard Optimization*, Springer-Verlag, Berlin/Heidelberg, 2006. 16
- 17 [28] P. Salamon, P. Sibani, R. Frost, *Facts, Conjectures, and Improvements for Simulated Annealing*, SIAM Monographs Mathematical Modeling and Computation, SIAM, 17
- 18 Philadelphia, 2002. 18
- 19 [29] S. Kirkpatrick, C.D. Gelatt Jr., M.P. Vecchi, *Science* 220 (1983) 671. 19
- 20 [30] N. Metropolis, A.W. Rosenbluth, M.N. Rosenbluth, A.H. Teller, E. Teller, *J. Chem. Phys.* 21 (1953) 1087. 20
- 21 [31] F. Bockisch, D. Liotard, J.C. Rayez, B. Duguay, *Int. J. Quant. Chem.* 44 (1992) 619. 21
- 22 [32] D.A. Liotard, *Int. J. Quant. Chem.* 44 (1992) 723. 22
- 23 [33] I. Andricioaei, J.E. Straub, *Comput. Phys.* 10 (1996) 449. 23
- 24 [34] A.T. Brünger, P.D. Adams, L.M. Rice, *Structure* 15 (1997) 325. 24
- 25 [35] T. Ogura, C. Sato, *J. Struct. Biol.* 156 (2006) 371. 25
- 26 [36] A. Niño, C. Muñoz-Caro, *Comput. Chem.* 18 (1994) 27. 26
- 27 [37] B. Podolsky, *Phys. Rev.* 32 (1928) 812. 27
- 28 [38] T.H. Cormen, C.E. Leiserson, R.L. Rivest, C. Stein, *Introduction to Algorithms*, second edition, The MIT Press, USA, 2001. 28
- 29 [39] M.A. Harthcock, J. Laane, *J. Mol. Spectrosc.* 91 (1982) 300. 29
- 30 [40] A. Niño, C. Muñoz-Caro, D.C. Moule, *J. Mol. Struct.* 318 (1994) 237. 30
- 31 [41] C. Muñoz-Caro, A. Niño, D.C. Moule, *Chem. Phys.* 186 (1994) 221. 31
- 32 [42] C. Muñoz-Caro, A. Niño, *Comput. Chem.* 18 (1994) 413. 32
- 33 [43] A. Niño, C. Muñoz-Caro, D.C. Moule, *J. Phys. Chem.* 98 (1994) 1519. 33
- 34 [44] C. Muñoz-Caro, A. Niño, D.C. Moule, *J. Chem. Soc. Faraday Trans.* 91 (1995) 399. 34
- 35 [45] A. Niño, C. Muñoz-Caro, *Comput. Chem.* 19 (1995) 371. 35
- 36 [46] A. Niño, C. Muñoz-Caro, D.C. Moule, *J. Phys. Chem.* 99 (1995) 8510. 36
- 37 [47] M.E. Castro, A. Niño, C. Muñoz-Caro, *Theor. Chem. Account.* 119 (2008) 343. 37
- 38 [48] W.H. Press, B.P. Flannery, S.A. Teukolsky, W.T. Vetterling, *Numerical Recipes. The Art of Scientific Computing*, Cambridge University Press, Cambridge, 2007. 38
- 39 [49] R. Fletcher, *Practical Methods of Optimization*, John Wiley & Sons, Toronto, 2000. 39
- 40 [50] M.E. Castro, A. Niño, C. Muñoz-Caro, *LNCS 5072* (2008) 1011. 40
- 41 [51] M.E. Castro, A. Niño, C. Muñoz-Caro, *Comput. Phys. Comm.* 180 (2009) 1183. 41
- 42 [52] M.L. Senent, *J. Phys. Chem. A* 108 (2004) 6286. 42
- 43 [53] M.L. Senent, M. Villa, F.J. Melendez, R. Dominguez-Gomez, *ApJ* 627 (2005) 567. 43
- 44 [54] U. Fuchs, G. Winnewisser, P. Groner, F.C. De Lucia, E. Herbst, *ApJS* 144 (2003) 277. 44
- 45 [55] C. Møller, M.S. Plesset, *Phys. Rev.* 46 (1934) 618. 45
- 46 [56] T.H. Dunning Jr., *J. Chem. Phys.* 90 (1989) 1007. 46
- 47 [57] M.J. Frisch, G.W. Trucks, H.B. Schlegel, G.E. Scuseria, M.A. Robb, J.R. Cheeseman, J.A. Montgomery Jr., T. Vreven, K.N. Kudin, J.C. Burant, J.M. Millam, S.S. Iyengar, J. Tomasi, 47
- 48 V. Barone, B. Mennucci, M. Cossi, G. Scalmani, N. Rega, G.A. Petersson, H. Nakatsuji, M. Hada, M. Ehara, K. Toyota, R. Fukuda, J. Hasegawa, M. Ishida, T. Nakajima, 48
- 49 Y. Honda, O. Kitao, H. Nakai, M. Klene, X. Li, J.E. Knox, H.P. Hratchian, J.B. Cross, C. Adamo, J. Jaramillo, R. Gomperts, R.E. Stratmann, O. Yazyev, A.J. Austin, R. Cammi, 49
- 50 C. Pomelli, J.W. Ochterski, P.Y. Ayala, K. Morokuma, G.A. Voth, P. Salvador, J.J. Dannenberg, V.G. Zakrzewski, S. Dapprich, A.D. Daniels, M.C. Strain, O. Farkas, D.K. Malick, 50
- 51 D. Rabuck, K. Raghavachari, J.B. Foresman, J.V. Ortiz, Q. Cui, A.G. Baboul, S. Clifford, J.A. Cioslowski, B.B. Stefanov, G. Liu, A. Liashenko, P. Piskorz, I. Komaromi, R.L. Martin, 51
- 52 D.J. Fox, T. Keith, M.A. Al-Laham, C.Y. Peng, A. Nanayakkara, M. Challacombe, P.M.W. Gill, B. Johnson, W. Chen, M.W. Wong, C. Gonzalez, J.A. Pople, *Gaussian 03 Program*, 52
- 53 Revision A.1, Gaussian, Inc., Pittsburgh, PA, 2003. 53
- 54 54
- 55 55
- 56 56
- 57 57
- 58 58
- 59 59
- 60 60
- 61 61
- 62 62
- 63 63
- 64 64
- 65 65
- 66 66